

Closed-Loop Transmit Diversity with Imperfect Feedback

Abdorreza Heidari, *Student Member, IEEE* and Amir K. Khandani, *Member, IEEE*

Abstract

The closed-loop transmit diversity technique is used to improve the performance of the downlink channel in MIMO communication systems. In these closed-loop systems, feedback delay and feedback error, as well as the sub-optimum reconstruction of the quantized feedback data, are the usual sources of deficiency. We address the efficient reconstruction of the beamforming weights in the presence of the feedback imperfections, by exploiting the residual redundancies in the feedback stream. Focusing on the issue of feedback delay, we propose two approaches to improve the performance. One is based on using a channel predictor at the receiver to compensate for the delay, and using a joint source-channel coding (JSCC) method similar to our previous work [2] to compensate for the feedback error. Another approach deals with the feedback imperfections in a unified reconstruction algorithm using JSCC techniques. Furthermore, we introduce the concept of Blind Antenna Verification which can substitute the conventional Antenna Weight Verification process without the need for any training data. The closed-loop mode 1 of the 3GPP standard is used as a benchmark, and the performance is examined within a Wideband-CDMA simulation framework. It is demonstrated that the proposed algorithms outperform the conventional methods at all mobile speeds, and are suitable for the implementation in practice.

Index Terms

Abdorreza Heidari and Amir K. Khandani are with the Coding and Signal Transmission Laboratory, Electrical and Computer Engineering Department, University of Waterloo, Waterloo, Ontario, Canada. E-mails: {reza,khandani}@cst.uwaterloo.ca .

This work is financially supported by Bell Canada, Communications and Information Technology Ontario (CITO), and Natural Sciences and Engineering Research Council of Canada (NSERC).

This paper in part [1] has been presented at the Conference on Information Sciences and Systems (CISS), March 2006.

Closed-loop transmit diversity, Channel State Information (CSI), MIMO closed-loop communication, imperfect feedback, feedback delay, feedback error, blind antenna weight verification, joint source-channel coding, WCDMA FDD, mode 1 of 3GPP, UMTS

I. INTRODUCTION

The increasing demand for internet and wireless services highlights the need for an increase in the capacity of the communication systems. Third generation of mobile communication, namely 3GPP [3] and 3GPP2 [4], have developed WCDMA [5] and CDMA2000, respectively, to address this trend. The improvement of the downlink capacity is one of the main challenges of the 3G systems, and closed-loop techniques are known to have the potential to solve the problem. As a well-known example, Transmit Adaptive Array [6] is part of the 3GPP standard with two transmit antennas at the base station and one receive antenna at the mobile unit, which uses the Channel State Information (CSI) to beamform the transmit signal.

In a downlink closed-loop system, the transmitter receives the required CSI through a limited-capacity feedback channel from the receiver. The feedback data is a low-rate bitstream resulting from rough quantization of the CSI at the receiver. There are three major imperfections which affect the closed-loop systems: feedback delay, feedback error, and sub-optimal reconstruction. Feedback delay has been shown to drastically affect the performance of closed-loop systems [7], [8], as the transmitter has to use outdated CSI. This problem gets worse as the mobile speed increases because the channel is changing more rapidly.

The feedback data is usually uncoded, or has a low-rate coding. Hence, a closed-loop scheme is sensitive to the errors in the feedback channel (see [2] and the references therein). Other than decreasing the closed-loop gain, feedback error causes another more serious problem. For decoding purposes, the receiver needs to know exactly what weights have been applied at the transmit antennas. However, the receiver is not normally aware of the location of the errors in the feedback channel, which causes mismatch at the receiver. This mismatch imposes an error floor on the system performance which is proportional to the feedback error rate as each feedback error can potentially result in symbol errors in the respective slot. In many

research works, an impractical assumption is made that the receiver somehow knows the exact transmitter weights at all times. Ratifying this problem in practice, an *Antenna-weight Verification* algorithm, also called *Antenna Verification* algorithm (AV), [9] is applied which needs some extra training data at the receiver for each user. There are a few works in the literature on the AV problem, such as [10], [11], [12]. These articles address the problem for the closed-loop modes¹ of the 3GPP standard, when the dedicated training data is available. In this article, we are interested in the AV problem without using any extra training, i.e, in a blind fashion. A recent paper [13] deals with a similar problem, however, for a single transmit-antenna selection system. Optimizing the signaling assignment, it has been shown that verification of the selected antenna at the receiver is crucial when the feedback is erroneous. Furthermore, a number of blind and non-blind AV methods have been proposed for the antenna selection system [13].

The reconstruction schemes used in closed-loop systems are usually not optimal due to simplifications of the algorithms, and ignoring the feedback error and delay. Our focus here is on Mode 1 of 3GPP [9] (as described in Section I-C) which only feeds back the phase information of the channel with a special quantization scheme. Despite all the imperfections, Mode 1 has a good performance at low mobile speeds, but it fails at higher speeds. In our previous work [2], the efficient reconstruction of beamforming weight in the presence of feedback error is addressed. Some joint source-channel techniques are used to improve the performance of Mode 1 of 3GPP, by taking advantage of the redundancy available in the CSI stream.

In this article, we consider the problem of feedback delay, as well as feedback error, in a closed-loop system. To solve this problem, we propose two approaches. One approach uses predicted channel values to compensate for the effect of feedback delay, and uses the JSCC method for the feedback error. In the other approach, a unified JSCC framework deals with the feedback imperfections. Exploiting the novel concept of Blind Antenna Verification, this method only uses the feedback bitstream and does not need any type of training data. The performance of the algorithms is examined in the framework of the closed-loop mode 1 of the 3GPP standard. For the channel model, we consider spatially-uncorrelated Rayleigh

¹Namely, mode 1 and mode 2. Mode 2 is no longer part of the 3GPP standard.

fading channels. In the simulations, we use a separate Jakes fading generator introduced in [14] for each channel. Here is a list of notations used in this paper: $[\cdot]^{(k)}$ refers to the k 'th element of a vector, $[\cdot]^H$ is the Hermitian transform, and \mathbb{C} is the set of complex numbers.

A. Beamforming

In a closed-loop system, channel input \mathbf{x} should be appropriately selected according to the channel state [15]. Controlling the channel input can be accomplished with a conventional beamformer which applies some weights to the transmitted signal for each antenna. Assuming two transmit antennas and one receive antenna, a beamforming scheme can be expressed as

$$\mathbf{x} = \mathbf{w}s, \quad (1)$$

where

$$\mathbf{w} = [w^{(1)}, w^{(2)}]^T \in \mathbb{C}^2, \quad (2)$$

and s is the transmitted symbol. It is assumed that $\|\mathbf{w}\|^2 = 1$, which means the beamformer does not change the transmit power. The received signal r is a complex number which is the superposition of the signals from different antennas, as well as the noise, i.e.,

$$r = \mathbf{h}^T \mathbf{w}s + \eta \quad (3)$$

$$= \left(\sum_{m=1}^2 h^{(m)} w^{(m)} \right) s + \eta. \quad (4)$$

In the decoding process, the combining complex variable is applied as [16]

$$z = v^H r = v^H \mathbf{h}^T \mathbf{w}s + v^H \eta, \quad (5)$$

where z is used to calculate the output LLR (Log-Likelihood Ratio) values. It has been shown [17] that to minimize the average probability of error in a MIMO system, \mathbf{w} and v must be jointly selected to maximize the instantaneous SNR. It could be concluded from (4) that $\text{SNR}_{inst} = |\mathbf{h}^T \mathbf{w}|^2 \frac{E_s}{N_0}$, where $E_s = E[|s|^2]$. Several schemes for selection of \mathbf{w} are introduced in the literature, for example refer to [15]. Later, we will discuss the calculation of v (i.e., Antenna Weight Verification) in Section III.

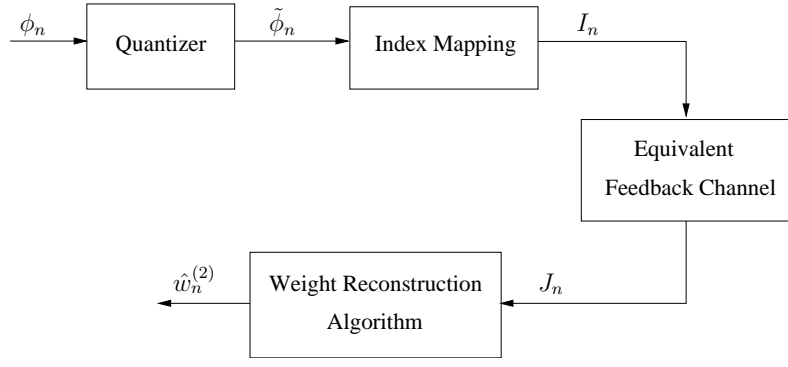


Fig. 1. Block diagram of a quantized co-phase feedback system

B. Quantized Co-phase Feedback

Figure 1 shows the block diagram of a quantized co-phase² feedback system. In the figure, $\phi_n = \angle h_n^{(2)} - \angle h_n^{(1)}$ is the co-phase information, $\tilde{\phi}_n$ is the quantized co-phase, and I_n is the respective index. I_n is sent through the feedback channel and J_n is received at the base station, possibly delayed and/or noisy. Here, a memoryless feedback channel is assumed.

At the transmitter, the phase information is used to calculate the beamforming weights, whereas the transmit power is constant. Hence, it is assumed $w_n^{(1)} = \frac{1}{\sqrt{2}}$ and $|w_n^{(2)}| = \frac{1}{\sqrt{2}}$. In an ideal co-phase feedback system, $\angle w_n^{(2)} = -\phi_n$.

C. Mode 1 of 3GPP

The closed-loop mode 1 of the 3GPP standard [9] is an example of the feedback system shown in Fig. 1. In mode 1, the quantization of the co-phase ϕ_n is subject to a special framing structure as shown in Fig. 2. Each (uplink) frame, which contains the feedback information, has a duration of 10 msec and includes 15 slots. Each slot contains a number of data symbols depending on the data rate. For each slot, one bit of feedback data is sent from the mobile unit which results in a feedback stream of 1500 bits per second. The feedback bit is determined by one of the two one-bit quantizers Q_0 and Q_1 , according to Fig. 2, where $Q_0 = \{0, \pi\}$ and $Q_1 = \{\pi/2, -\pi/2\}$. Showing the relative place of each slot in a frame, we use a framed time index, $\tau = n \bmod 15$, hence in a frame, $\tau = 0, 1, \dots, 14$.

²The term co-phase refers to the phase difference between the two channels.

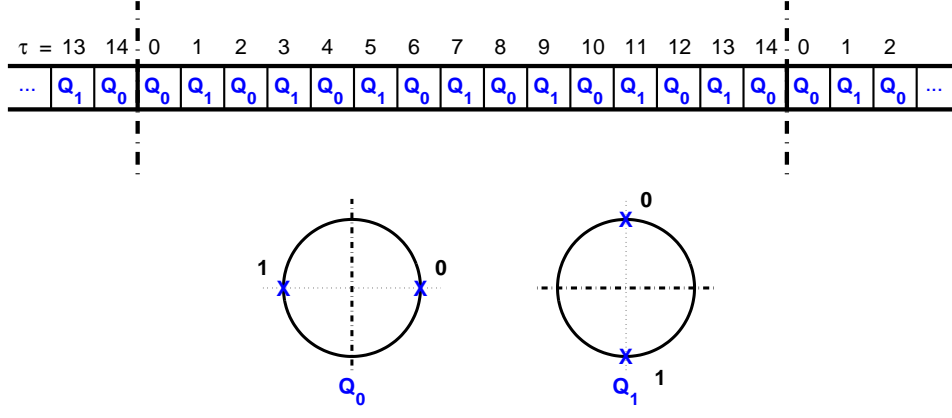


Fig. 2. The framing structure and the quantizers of mode 1 of 3GPP

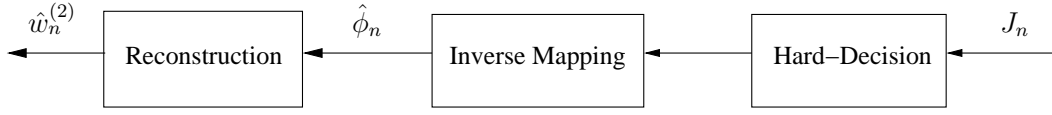


Fig. 3. Block diagram of the weight reconstruction for mode 1 of 3GPP

At the base station, after a hard-decision unit, the received feedback data bits are mapped to $\hat{\phi}_n$ phase stream according to Fig. 2, i.e., $\hat{\phi}_n \in Q_{\tau \bmod 2}$. The weight $w_n^{(2)}$ is constructed from the two recent phases, one from a Q_0 slot and one from a Q_1 slot. The reconstruction scheme can be shown as

$$\hat{w}_n^{(2)} = \begin{cases} \frac{1}{2}(e^{j\hat{\phi}_n} + e^{j\hat{\phi}_{n-1}}), & \tau \neq 0 \\ \frac{1}{2}(e^{j\hat{\phi}_n} + e^{j\hat{\phi}_{n-2}}), & \tau = 0. \end{cases} \quad (6)$$

Note that at each time, equation (6) selects the $\hat{w}_n^{(2)}$ from a set of 4 predefined weights. This construction also guarantees that $|\hat{w}_n^{(2)}| = \frac{1}{\sqrt{2}}$ for all n .

It is observed from Fig. 2 that $\tilde{\phi}_n$ (and similarly $\hat{\phi}_n$) can attain one of four values, $\tilde{\phi}_n \in \{-\pi/2, 0, \pi/2, \pi\}$. Therefore, index I_n could be defined as $I_n \in \{0, 1, 2, 3\}$, respectively. It is notable that these 2-bit symbols are constructed from the 1-bit feedback and the time information τ . Furthermore, equation (6) shows that the weight reconstruction block of mode 1 can be depicted as shown in Fig. 3. It is observed that the weight reconstruction algorithm has been separated into different parts in the standard, and can be potentially improved through a joint design, i.e., calculation of $\hat{w}_n^{(2)}$ directly from the sequence of J_n .

II. EFFICIENT RECONSTRUCTION OF THE BEAMFORMING WEIGHT

In the sequel, we assume the framing structure and the quantization scheme of the closed-loop mode 1 of the 3GPP standard [9], as described in the previous section. However, our approach can be used for any other feedback scheme as well.

A. MMSE Solution in the Presence of Feedback Delay and Error

In the previous work [2], [18], the MMSE algorithm in the presence of noisy feedback is introduced. The best algorithm is obtained when soft-output is used (i.e., assuming that J_n is available before a hard-decision operation), and it is called *SoftNMMSE* (Soft-Normalized-MMSE). In the following, a similar approach is pursued when the feedback data is delayed as well.

Assuming a delay of d symbols in the feedback channel (d is a non-negative integer), the sequence $\underline{J}_{n-d} = [J_1, J_2, \dots, J_{n-d}]$ is available at the base station at time n . The fundamental theorem of estimation states that given \underline{J}_{n-d} ,

$$\hat{w}_n^{(2)} = E [w_n^{(2)} | \underline{J}_{n-d}] \quad (7)$$

is the minimum mean-squared error (MMSE) estimate of the weight $w_n^{(2)}$. Similar to what is shown in [19], the formula can be approximated by the following form:

$$\hat{w}_n^{(2)} = \sum E [w_n^{(2)} | \underline{I}_n^{n-\mu+1}] P (\underline{I}_n^{n-\mu+1} | \underline{J}_{n-d}), \quad (8)$$

where the summation is over all the possible μ -fold sequences of $\underline{I}_n^{n-\mu+1} = [I_{n-\mu+1}, \dots, I_{n-1}, I_n]$. In (8), $E [w_n^{(2)} | \underline{I}_n^{n-\mu+1}]$ is a codebook, and the probability part can be computed as explained in Section II-A1.

We are dealing with the estimation of a complex variable with a constant amplitude, as $|\hat{w}_n^{(2)}| = \frac{1}{\sqrt{2}}$. However, there is no control on the amplitude of $\hat{w}_n^{(2)}$ in (7) and (8). Hence, we need an MMSE estimator with a constant amplitude, which is introduced in a lemma in [2] and is called NMMSE (Normalized-MMSE). According to the lemma, the antenna weight can be calculated using the MMSE solution of (7)

or (8) as

$$\hat{w}_n^{(2)-normal} = \frac{1}{\sqrt{2}} \frac{\hat{w}_n^{(2)}}{|\hat{w}_n^{(2)}|}. \quad (9)$$

1) *Markov Model*: For capturing the residual redundancies [20] in the feedback stream, we assume that the bitstream follows a Markov model of order γ . A trellis structure is set up based on the Markov model to exploit the redundancies. The states of the trellis are defined as $S_n = \underline{I}_n^{n-\gamma+1}$. The trellis is specified by the probabilities of the state transitions, $P(S_n|S_{n-1})$, which are the A Priori Probabilities (APP) of the Markov model.

2) *Calculation of the A Posteriori Probabilities at the Transmitter*: The probability $P(\underline{I}_n^{n-\mu+1} | \underline{J}_{n-d})$ in (8) could be calculated by using the state probabilities given the received feedback data, $P(S_n|\underline{J}_{n-d})$. In the absence of feedback delay, this calculation reduces to $P(S_n|\underline{J}_n)$ as in [2] which is the estimation of the state probabilities at time n given the feedback symbols up to time n . In the following, we present a recursive algorithm for calculation of $P(S_n|\underline{J}_{n-d})$. Note that this formulation has a predictive nature as well, because the last d feedback symbols are not available due to the feedback delay. In other words, this is a joint prediction and estimation method, and so the resulting algorithm is called *SoftNMMSE-JP*, where *JP* stands for Joint Prediction.

Let

$$\begin{aligned} P(S_n|\underline{J}_{n-d}) &= C_1 \cdot P(S_n, \underline{J}_{n-d}) \\ &= C_1 \cdot P(\underline{J}_{n-d-1}) \cdot P(S_n|\underline{J}_{n-d-1}) \\ &\quad \cdot P(J_{n-d}|S_n, \underline{J}_{n-d-1}) \end{aligned} \quad (10)$$

$$= C_2 \cdot P(S_n|\underline{J}_{n-d-1}) \cdot P(J_{n-d}|I_{n-d}) \quad (11)$$

for $d \leq \gamma - 1$, where C_1 and C_2 are normalizing variables. The term $P(S_n|\underline{J}_{n-d-1})$ can be written as follows

$$P(S_n|\underline{J}_{n-d-1}) =$$

$$\begin{aligned}
& \sum_{\underline{S}_{n-1}} \cdots \sum P(S_n | \underline{S}_{n-1}, \underline{J}_{n-d-1}) \cdot P(\underline{S}_{n-1} | \underline{J}_{n-d-1}) \\
&= \sum_{\underline{S}_{n-1}} \cdots \sum P(S_n | S_{n-1}) \cdot P(S_{n-1}, \underline{S}_{n-2} | \underline{J}_{n-d-1}) \\
&= \sum_{S_{n-1}} P(S_n | S_{n-1}) \cdot \sum_{\underline{S}_{n-2}} \cdots \sum P(S_{n-1}, \underline{S}_{n-2} | \underline{J}_{n-d-1}) \\
&= \sum_{S_{n-1}} P(S_n | S_{n-1}) \cdot P(S_{n-1} | \underline{J}_{n-d-1}). \tag{12}
\end{aligned}$$

Therefore, $P(S_n | \underline{J}_{n-d})$ can be calculated recursively as

$$\begin{aligned}
P(S_n | \underline{J}_{n-d}) &= C_2 \cdot P(J_{n-d} | I_{n-d}) \\
&\quad \cdot \sum_{S_{n-1}} P(S_n | S_{n-1}) \cdot P(S_{n-1} | \underline{J}_{n-d-1}). \tag{13}
\end{aligned}$$

Another approach to overcome the feedback delay is introduced in the following section.

B. Channel Prediction at the Receiver

If the receiver calculates the feedback symbols by using the future channel states, it can cancel out the effect of the delay in the feedback channel. This approach can be implemented by using d -step predicted values of the channel coefficients, and these values can be computed by applying a short-range fading prediction algorithm [21], [22] to the current channel values. Here we use an Auto Regressive (AR) model of order 3 to predict the fading samples, and *SoftNMMSE* is used to deal with the feedback error. The resulting algorithm is called *SoftNMMSE-LP* where *LP* stands for Linear Prediction.

In practice, channel coefficients are estimated using some pilots, training bits, etc. which usually introduce some error in the available channel coefficients. Note that these channel estimates are used to generate feedback symbols, calculate the LLR values for the decoding process, etc. Therefore, the quality could have a direct impact on the overall performance of a closed-loop system. Here, the channel estimation error is modelled as an Additive White Gaussian Noise (AWGN), and SNR_z is defined as the ratio of the average channel fading power, $E[|h_n|^2]$, to the noise power. The effect of SNR_z on the performance of different algorithms is examined in the simulations.

III. ANTENNA WEIGHT VERIFICATION

When an error occurs in the feedback channel, an incorrect antenna weight (i.e., beamforming weight) vector is applied at the transmitter, which leads to two consequences. First, the received signal power is smaller [23], because a non-optimum weight is applied. However, our simulations show that the performance degradation due to this effect is rather small. The second consequence is more serious: Each time a feedback error occurs, the mobile station does not know the actual antenna weight vector that is applied at the base station. Since the mobile station obtains the dedicated (i.e., user-specific) channel estimate by combining the estimates for individual antennas from common pilots with the assumed weight vector used at the base station, this can cause significant dedicated channel estimation error, henceforth error in calculation of the combining variable v , resulting in some error floor in the performance. To minimize this effect, a technique called Antenna Weight Verification (AV) [10] has been suggested. In this method, some extra preamble bits are transmitted to each user, and these are used to estimate the dedicated channel which includes the effect of possible feedback errors.

In the next section, we introduce a novel technique called Blind Antenna Verification (BAV) which does not need any extra preamble bits. This blind method processes the feedback symbols, which means that the proposed method has a low complexity in comparison with symbol-based³ blind approaches (such as the blind selection verification methods introduced in [13]). Using the proposed BAV in conjunction with the *SoftNMMSE-JP* algorithm provides an efficient closed-loop algorithm in the presence of feedback imperfections, as shown in the numerical results.

³By a symbol-based method, we mean that a method that needs to perform calculations on the sequence of data symbols. On the other hand, the proposed method in this article only needs a slot-by-slot calculation. The complexity of these two approach is proportional to symbol rate and feedback rate, respectively.

A. Blind Antenna Verification

Consider Fig. 4. At the transmitter, the best estimate of the optimum beamforming weight, in the MMSE sense, is

$$\hat{\mathbf{w}}_n = E[\mathbf{w}_n | \underline{J}_{n-d}]. \quad (14)$$

Transmitter applies the weight to the transmit signals. At the receiver, an estimate of $\hat{\mathbf{w}}_n$ is required for the decoding process, for example, for the calculation of v in (5). Assume that the receiver uses $\tilde{\mathbf{w}}_n$. Hence, $\tilde{\mathbf{w}}_n$ needs to be as close to $\hat{\mathbf{w}}_n$ as possible. In the following, we introduce a theorem to address this problem. Two lemmas are introduced beforehand which are used to prove the theorem.

Lemma 1: The following sequence

$$\mathbf{w}_n \leftrightarrow \underline{I}_{n-d} \leftrightarrow \underline{J}_{n-d} \quad (15)$$

constitutes a Markov chain.

Proof: See Appendix A. ■

Lemma 2: Assume that $X \leftrightarrow Y \leftrightarrow Z$ constitutes a Markov chain. Then,

$$E[E[X|Y]|Z] = E[X|Z]. \quad (16)$$

Proof: See Appendix B. ■

Note that the inner $E[\cdot]$ of the left side of (16) and the $E[\cdot]$ of the right side are with respect to X , and the outer $E[\cdot]$ of the left side is with respect to Y .

Theorem 1 (Joint Beamforming and Blind Antenna Verification): In a closed-loop system, the following criteria are desired:

- 1) Select $\tilde{\mathbf{w}}_n$ to

$$\text{minimize } E\|\tilde{\mathbf{w}}_n - \mathbf{w}_n\|^2 \quad (17)$$

given \underline{I}_{n-d} which is available at the receiver.

- 2) Select $\hat{\mathbf{w}}_n$ to

$$\text{minimize } E\|\hat{\mathbf{w}}_n - \tilde{\mathbf{w}}_n\|^2 \quad (18)$$

given \underline{J}_{n-d} which is available at the transmitter.

The following system satisfies both criteria:

$$\tilde{\mathbf{w}}_n = E[\mathbf{w}_n | \underline{I}_{n-d}], \quad (19)$$

$$\hat{\mathbf{w}}_n = E[\mathbf{w}_n | \underline{J}_{n-d}]. \quad (20)$$

Proof: From criterion 1, according to the fundamental theorem of estimation (19) is obtained. The transmitter should find an estimate of $\tilde{\mathbf{w}}_n$ as given in (18). Let us call this weight $\hat{\tilde{\mathbf{w}}}_n$. Again, by using the fundamental theorem of estimation, from criterion 2 we can write

$$\hat{\tilde{\mathbf{w}}}_n = E[\tilde{\mathbf{w}}_n | \underline{J}_{n-d}]. \quad (21)$$

In the following, we will show that $\hat{\tilde{\mathbf{w}}}_n = \hat{\mathbf{w}}_n$ where $\hat{\mathbf{w}}_n$ is introduced in (20), and this concludes the proof.

According to Lemma 1,

$$\mathbf{w}_n \leftrightarrow \underline{I}_{n-d} \leftrightarrow \underline{J}_{n-d} \quad (22)$$

constitutes a Markov chain. Hence we can write

$$\hat{\tilde{\mathbf{w}}}_n = E[\tilde{\mathbf{w}}_n | \underline{J}_{n-d}] \quad (23)$$

$$= E[E[\mathbf{w}_n | \underline{I}_{n-d}] | \underline{J}_{n-d}] \quad (24)$$

$$= E[\mathbf{w}_n | \underline{J}_{n-d}] \quad (25)$$

$$= \hat{\mathbf{w}}_n, \quad (26)$$

where Lemma 2 is used to derive (25). The result shows that if the transmitter uses (20), and the receiver uses (19), both criteria are satisfied. ■

Note that theorem 1 does not explicitly use the optimal beamforming criterion (i.e., minimize $E\|\hat{\mathbf{w}}_n - \mathbf{w}_n\|^2$, as is used in [2]), however this criterion is satisfied by (20). This means that beamforming goal and AV goal are jointly achieved by using the theorem. This method does not need any dedicated (i.e., user-specific) training sequence at the receiver and so it is a blind solution for the AV problem. For the implementation

of the solution introduced in Theorem 1, the receiver calculates (19) which could be done similar to (8). However, it does not need any trellis processing because the probabilities are fixed. The required $P(S_n|\underline{I}_{n-d})$ can be calculated as shown in Appendix C.

IV. NUMERICAL RESULTS

The block diagram of the simulated feedback system is shown in Fig. 4. The simulation parameters are summarized in Table I. The feedback bitstream is BPSK modulated (uncoded) and added with White Gaussian Noise with the variance of $\sigma_n^2 = 0.370$ (equivalent to the feedback error of 5%). The following algorithms are compared: *Standard*, *SoftNMMSE-JP-BAV*, *SoftNMMSE-LP*, and *SoftNMMSE-IP*. *Standard* refers to the closed-loop mode 1 of the 3GPP standard, as explained in Section I-C. The algorithm *SoftNMMSE-JP-BAV* is an implementation of Theorem 1 which is a combination of the Joint Prediction approach of Section II and Blind Antenna Verification. The algorithm *SoftNMMSE-LP* uses the approach in Section II-B which applies a linear predictor of order 3 for channel prediction. Finally, the algorithm *SoftNMMSE-IP* (where “IP” stands for Ideal Channel Prediction) uses the same approach as Section II-B, but assumes that the required future channel coefficients are perfectly available without the effect of channel estimation and channel prediction errors. Therefore, *SoftNMMSE-IP* can be considered as a performance bound for dealing with feedback delay. It is notable that *SoftNMMSE-JP-BAV* and *SoftNMMSE-LP* are enhancements to the closed-loop mode 1 of 3GPP, and they are compatible with the standard.

Fig. 5 shows the FER performance curves versus transmit SNR at four different mobile speeds ($V=1, 5, 25$, and 100 kmph), for $\text{SNR}_z = 40$ dB representing the case where the channel estimation has a good quality (for example, when powerful channel pilots are available). Similarly, Fig. 6 shows the FER performance curves for $\text{SNR}_z = 10$ dB representing the case with poor channel estimation quality (for example, when blind channel estimation is used at the receiver).

It is observed that both proposed approaches significantly outperform the *Standard* algorithm at all mobile speeds. For the case of high SNR_z , the channel prediction approach acts better than the joint approach which only uses the feedback bitstream. However, when SNR_z is low, the joint approach acts

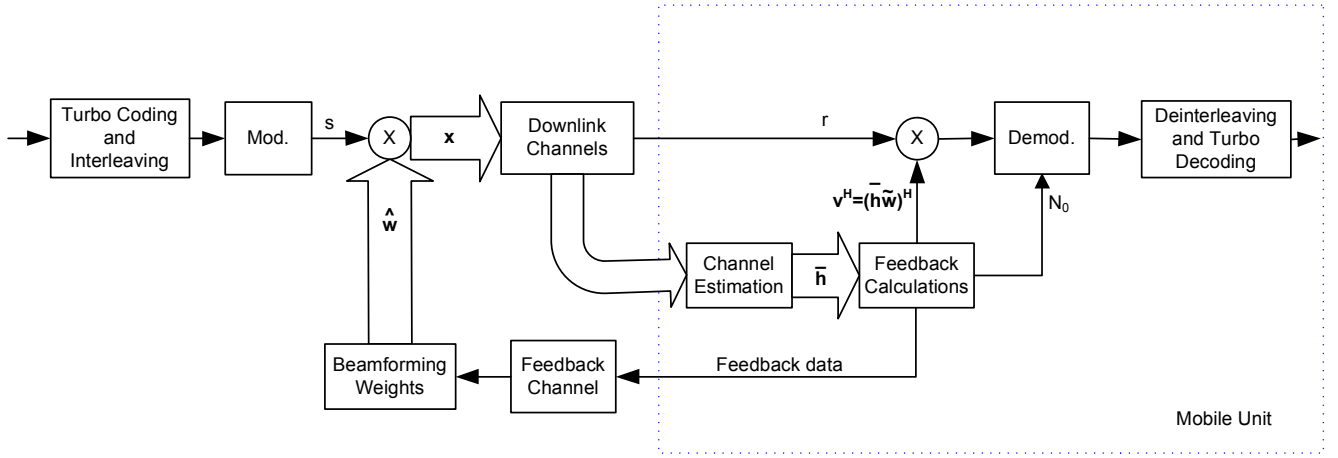


Fig. 4. Block diagram of our feedback system

Carrier Frequency	2.15 GHz
Modulation	QPSK
Transmitter	2 Antennas
Receiver	1 Antenna
Data Rate	15000 bps
Feedback Rate	1500 bps
Channel Coding	Turbo Code
Code Rate	1/3
Frame Length	300 (20 mSec)
Bit Interleaving	One Frame
Power Control	Not applied
Feedback Delay	2 slots
Feedback Noise Variance	0.370

TABLE I

SIMULATION PARAMETERS

better, since the predicted channel values are not very accurate in this case.

For high SNR_z and low mobile speeds, both approaches have the same performance and offer about 1 dB gain over the *Standard* algorithm. When the mobile speed is low, channel is changing slowly and the roughly quantized CSI has enough information about the channel. Also, the channel prediction algorithms

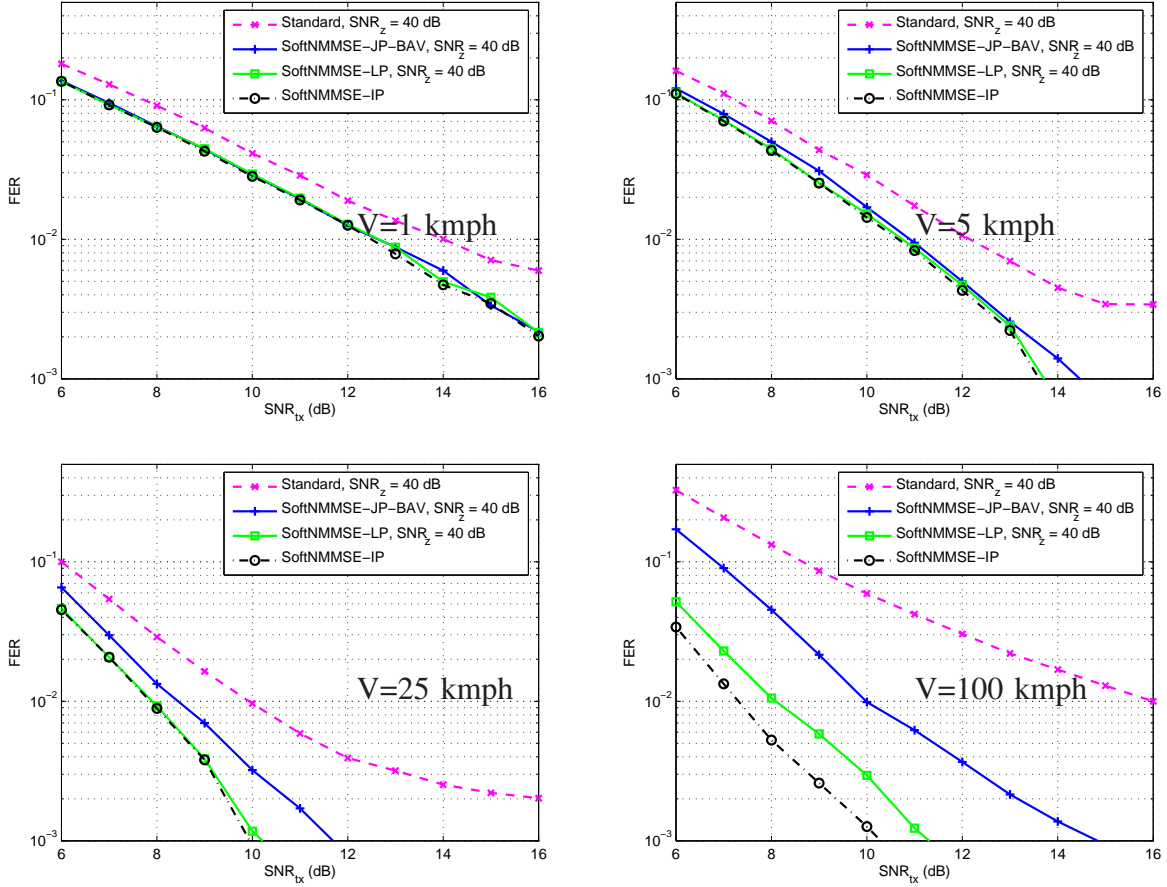


Fig. 5. FER performance at $\text{SNR}_z = 40$ dB

act very well as the channel values have significant time-correlation. In other words, the effect of feedback delay vanishes for low mobile speeds. Therefore, as it is observed in Fig. 5 for $V=1$ kmph, both approach touch the “*SoftNMMSE-IP*” performance. As the mobile speed increases, the increasing effect of feedback delay causes the performance curves to split.

It is observed that at high mobile speeds, our joint approach significantly outperforms the *Standard* algorithm, for both poor and good quality of channel estimation. This shows that our joint prediction algorithm can be used to increase the range of mobile speeds where the closed-loop algorithm can be effectively applied. The algorithm only needs the calculations once per each feedback slot (i.e., the total complexity is proportional to the feedback rate which is much less than the data symbol rate), and the

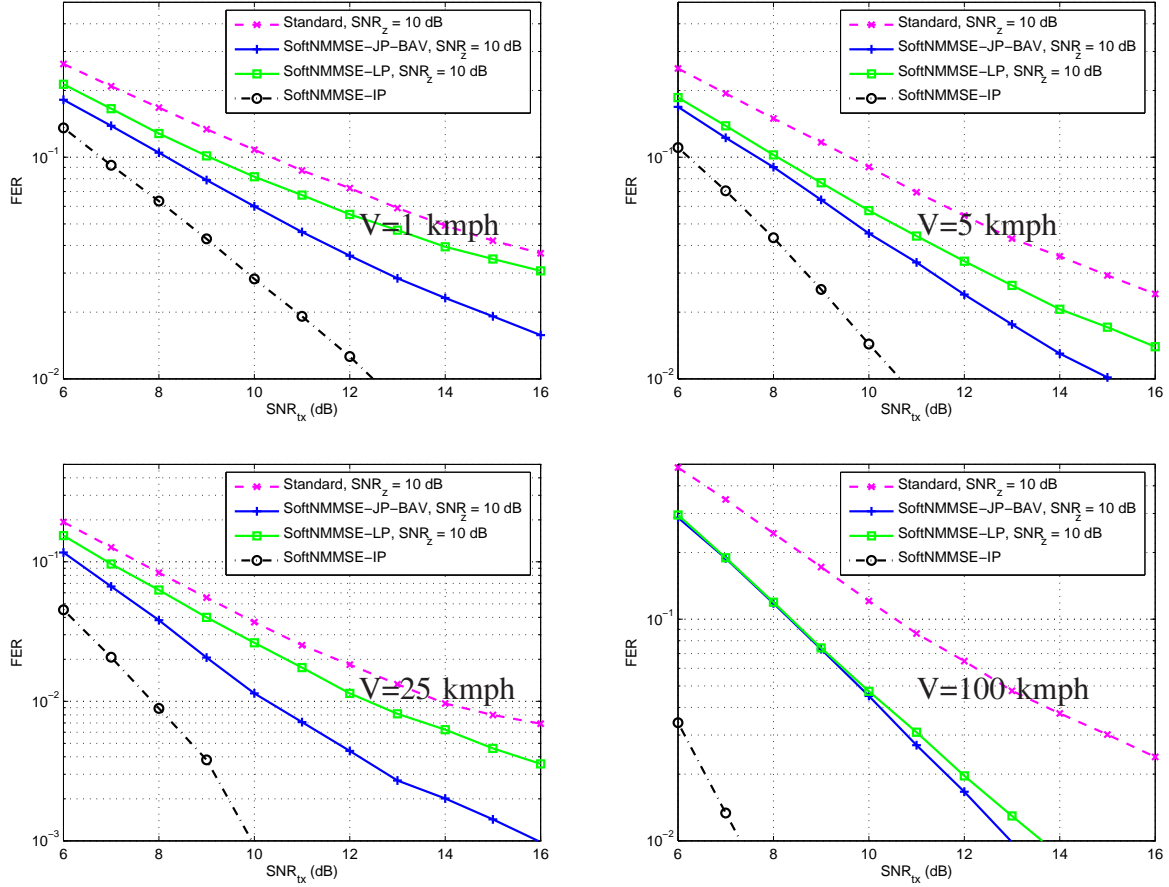


Fig. 6. FER performance at $\text{SNR}_z = 10$ dB

algorithm has a reasonable complexity, mostly needed at the base station. Both approach proposed in this paper are similarly applicable to any other MIMO closed-loop system.

APPENDIX A

PROOF OF LEMMA 1

Using the data processing theorem, we know that

$$\underline{\mathbf{w}}_n \leftrightarrow \underline{I}_{n-d} \leftrightarrow \underline{J}_{n-d} \quad (27)$$

forms a Markov chain, because the feedback sequence \underline{I}_{n-d} is calculated from the weight sequence $\underline{\mathbf{w}}_n$ at the receiver, and \underline{J}_{n-d} , which is received at the transmitter after passing through the feedback channel,

is an (stochastically) impaired version of \underline{I}_{n-d} . Therefore, for the conditional PDF's, it can be written

$$f(\underline{\mathbf{w}}_n | \underline{I}_{n-d}, \underline{J}_{n-d}) = f(\underline{\mathbf{w}}_n | \underline{I}_{n-d}). \quad (28)$$

Now, the following integration of both sides

$$\begin{aligned} \int \cdots \int_{\underline{\mathbf{w}}_{n-1}} f(\underline{\mathbf{w}}_n | \underline{I}_{n-d}, \underline{J}_{n-d}) d\underline{\mathbf{w}}_{n-1} = \\ \int \cdots \int_{\underline{\mathbf{w}}_{n-1}} f(\underline{\mathbf{w}}_n | \underline{I}_{n-d}) d\underline{\mathbf{w}}_{n-1}, \end{aligned} \quad (29)$$

results in

$$f(\underline{\mathbf{w}}_n | \underline{I}_{n-d}, \underline{J}_{n-d}) = f(\underline{\mathbf{w}}_n | \underline{I}_{n-d}), \quad (30)$$

meaning that

$$\underline{\mathbf{w}}_n \leftrightarrow \underline{I}_{n-d} \leftrightarrow \underline{J}_{n-d} \quad (31)$$

is a Markov chain.

APPENDIX B

PROOF OF LEMMA 2

As a property of a Markov chain,

$$f(x|y, z) = f(x|y), \quad (32)$$

where $f(\cdot)$ is the PDF of the respective random variable. Hence,

$$E_Y [E_X[X|Y]|Z] = \quad (33)$$

$$\int \left(\int x f(x|y) dx \right) f(y|z) dy \quad (34)$$

$$= \int \int x f(x|y) f(y|z) dx dy \quad (35)$$

$$= \int \int x f(x|y, z) f(y|z) dx dy \quad (36)$$

$$= \int \int x f(x, y|z) dx dy \quad (37)$$

$$= \int x f(x|z) dx \quad (38)$$

$$= E_X[X|Z]. \quad (39)$$

APPENDIX C

DERIVATION OF $P(S_n|I_{n-d})$ FOR RECEIVER

We can write

$$P(S_n|I_{n-d}) = P(S_n|\underline{S}_{n-d}) \quad (40)$$

$$= P(S_n|S_{n-d}), \quad (41)$$

where $P(S_n|S_{n-d})$ is the d -step transition probability which is calculated once as follows

$$P(S_n|S_{n-d}) = P(S_n|\underline{S}_{n-d}) \quad (42)$$

$$= \sum_{\underline{S}_{n-1}^{n-d-1}} \cdots \sum P(S_n|S_{n-1}) \cdot P(S_{n-1}|S_{n-2}) \cdots P(S_{n-d-1}|S_{n-d}). \quad (43)$$

REFERENCES

- [1] A. Heidari, and A. K. Khandani, "Improved Closed-Loop Communication in the Presence of Feedback Delay and Error," *Conference on Information Sciences and Systems (CISS)*, pp. 289–294, Mar. 2006.
- [2] A. Heidari, F. Lahouti, and A. K. Khandani, "Improved Reconstruction of Channel State Information for Low-Rate Feedback Schemes," *IEEE Trans. on Vehicular Technology (to appear)*. Available at <http://cst.uwaterloo.ca/~reza>.
- [3] "The 3GPP website: <http://www.3gpp.org>."
- [4] "The 3GPP2 website: <http://www.3gpp2.org>."
- [5] 3GPP Technical Specification, "UMTS Physical Layer: General Description," *ETSI TS 125 201 V6.0.0*, Dec. 2003.
- [6] R. T. Derryberry et al., "Transmit Diversity in 3G CDMA Systems," *IEEE Communications Magazine*, pp. 68–75, Apr. 2002.
- [7] E. N. Onggosanusi et al., "Performance Analysis of Closed-Loop Transmit Diversity in the Presence of Feedback Delay," *IEEE Trans. on Communications*, pp. 1618–1630, Sept. 2001.
- [8] J. Du, Y. Li, D. Gu, A. F. Molisch, J. Zhang, "Estimation of performance loss due to delay in channel feedback in MIMO systems," *IEEE Vehicular Technology Conference*, pp. 1619–1622, Sept. 2004.
- [9] 3GPP Technical Specification, "UMTS Physical Layer Procedures (FDD)," *ETSI TS 125 214 V6.0.0*, Dec. 2003.
- [10] A. Seeger and M. Sikora, "Antenna Weight Verification for Closed-Loop Transmit Diversity," *IEEE Global Telecommunications Conference (GLOBECOM)*, pp. 1124–1129, Dec. 2003.

- [11] S. Nagaraj and P. Monogioudis, "Antenna verification for closed loop transmit diversity in UMTS," *IEEE Vehicular Technology Conference*, pp. 3792 – 3796, Sept. 2004.
- [12] A. Serratore and E. Messina, "Analytical Evaluation And Performance Analysis Of Antenna Verification Algorithm In Closed Loop Antenna Diversity," *The 9th Asia-Pacific Conference on Communications (APCC)*, pp. 9–14, Sept. 2003.
- [13] Y. Li, N. B. Mehta, A. F. Molisch, J. Zhang, "Optimal Signaling and Selection Verification for Single Transmit-Antenna Selection," *IEEE Trans. on Communications*, pp. 778–789, Apr. 2007.
- [14] M. F. Pop and C. Beaulieu, "Limitations of Sum-of-Sinusoids Fading Channel Simulators," *IEEE Trans. on Communications*, pp. 699–708, Apr. 2001.
- [15] A. Narula, M. J. Lopez, M. D. Trott, and G. W. Wornell, "Efficient Use of Side Information In Multiple-Antenna Data Transmission Over Fading Channels," *IEEE Journal on selected Areas in Communications*, pp. 1423–1436, Oct. 1998.
- [16] J. G. Proakis, *Digital Communications*. Mc-Graw Hill International Editions, 2001.
- [17] P. A. Dighe, R. K. Mallik, and S. S. Jamuar, "Analysis of Transmit-Receive Diversity in Rayleigh Fading," *IEEE Trans. on Communications*, pp. 694–703, Apr. 2003.
- [18] A. Heidari, F. Lahouti, and A. K. Khandani, "Improved Reconstruction of Channel State Information in 3GPP," *Vehicular Technology Conference (VTC'F05), Dallas, Texas, USA*, Sept. 2005.
- [19] F. Lahouti and A. K. Khandani, "Reconstruction of Predictively Encoded Signals over Noisy Channels Using a Sequence MMSE Decoder," *IEEE Trans. on Communications*, pp. 1292–1301, Aug. 2004.
- [20] K. Sayood and J. C. Brokenhagen, "Use Of Residual Redundancy In The Design Of Joint Source-Channel Coders," *IEEE Trans. on Communications*, pp. 838–846, 1991.
- [21] A. Duel-Hallen, S. Hu, H. Hallen, "Long Range Prediction of Fading Signals: Enabling Adaptive Transmission for Mobile Radio Channels," *IEEE Signal Processing Magazine*, May 2000.
- [22] A. Heidari, F. Lahouti, D. McAvoy, and A. K. Khandani, "Improvement of Closed-loop Communication Systems in the Presence of Feedback Imperfections," tech. rep., Bell Mobility, Dec. 2005.
- [23] H. Gerlach, "SNR Loss due to Feedback Quantization and Errors in Closed Loop Transmit Diversity Systems," *The 13th IEEE International Symposium on Personal, Indoor and Mobile Radio Communications (PIMRC)*, pp. 2117–2120, Sept. 2002.